

Two-Photon Fluorescence Coincidence Analysis: Rapid Measurements of Enzyme Kinetics

Katrin G. Heinze,* Markus Rarbach,† Michael Jahnz,* and Petra Schwille*

*Experimental Biophysics Group, Max-Planck-Institute for Biophysical Chemistry, D-37077 Göttingen, Germany, and

†DIREVO Biotech AG, D-50829 Köln, Germany

ABSTRACT Dual-color fluorescence cross-correlation analysis is a powerful tool for probing interactions of different fluorescently labeled molecules in aqueous solution. The concept is the selective observation of coordinated spontaneous fluctuations in two separate detection channels that unambiguously reflect the existence of physical or chemical linkages among the different fluorescent species. It has previously been shown that the evaluation of cross-correlation amplitudes, i.e., coincidence factors, is sufficient to extract essential information about the kinetics of formation or cleavage of chemical or physical bonds. Confocal fluorescence coincidence analysis (CFCA) (Winkler et al., *Proc. Natl. Acad. Sci. U.S.A.* 96:1375–1378, 1999) emphasizes short analysis times and simplified data evaluation and is thus particularly useful for screening applications or measurements on live cells where small illumination doses need to be applied. The recent use of two-photon fluorescence excitation has simplified dual- or multicolor measurements by enabling the simultaneous excitation of largely different dye molecules by a single infra-red laser line (Heinze et al., *Proc. Natl. Acad. Sci. U.S.A.* 97:10377–10382, 2000). It is demonstrated here that a combination of CFCA with two-photon excitation allows for minimization of analysis times for multicomponent systems down to some hundreds of milliseconds, while preserving all known advantages of two-photon excitation. By introducing crucial measurement parameters, experimental limits for the reduction of sampling times are discussed for the special case of distinguishing positive from negative samples in an endonucleolytic cleavage assay.

INTRODUCTION

Fluorescence correlation spectroscopy (FCS) (Magde et al., 1972; Elson and Rigler, 2001; Schwille, 2001a) and related confocal techniques currently play an important role in the investigation of dynamics and interactions of biomolecules at the single-molecule level (Eigen and Rigler, 1994; Weiss, 1999; Schwille and Kettling, 2001). The main concept of these techniques is the temporal analysis of laser-induced fluorescence fluctuations within a small open volume element of approximately one femtoliter (10^{-15} l), defined by the illuminated focal spot of a high-resolution microscope objective. Standard one-color FCS allows for sensitive probing of molecular concentrations and mobility (Elson and Magde, 1974; Aragón and Pecora, 1976; Koppel et al., 1976; Rigler et al., 1993), and, consequently, all kinds of interactions that change these parameters, such as binding and unbinding to large reaction partners or immobile structures (Kinjo and Rigler, 1995; Schwille et al., 1997a), and particle aggregation (Palmer and Thompson, 1987). Another popular field of FCS applications is the study of intramolecular fluctuations associated with intermittent emission behavior, often referred to as “blinking” or “flickering” on fast time scales compared to the molecular residence time in the illuminated volume (Magde et al., 1972). This kind of kinetic analysis reveals information about the

molecular microenvironment, via triplet state population (Widengren et al., 1995; Widengren and Rigler, 1998) or reversible protonation (Haupts et al., 1998). It may also reflect reversible binding or conformational changes of the biomolecules under study, e.g., if these processes induce quenching of the fluorescent labels (Bonnet et al., 1998), or changes in the fluorescence resonance energy transfer efficiency between two labels attached to different sites of a single molecule (Wallace et al., 2000; Schwille, 2001b; Widengren et al., 2001).

To probe the interactions between two different molecular species, dual-color cross-correlation analysis (Schwille et al., 1997b; Schwille, 2001b) has proven to be far superior to conventional FCS due to its inherent measurement selectivity. The underlying idea is to label both species under study with spectrally distinct dyes, and to specifically record coordinated spontaneous fluctuations in the two respective detection channels, which unambiguously reflect the existence of physical or chemical linkages between the two fluorophores. Thus, dual-color cross-correlation analysis can be considered a dynamic analog to co-localization techniques frequently used in fluorescence imaging, with the important advantage of considerably reduced false-positive signals due to the extremely low probability of coordinated fluctuations of two fully independent measurement parameters. Dual-color cross-correlation analysis has been applied to probe kinetics of irreversible association (Schwille et al., 1997b), the polymerization of DNA in polymerase chain reaction (Rigler et al., 1998), the early aggregation events in prion protein PrP^{Sc} rod formation (Bieschke and Schwille, 1997; Bieschke et al., 2000), binding of DNA

Submitted January 2, 2002 and accepted for publication May 7, 2002.

Address reprint requests to Petra Schwille, Experimental Biophysics Group, Max-Planck-Institute for Biophysical Chemistry, Am Fassberg 11, D-37077 Göttingen, Germany. Tel.: +49-551-201-1165; Fax: +49-551-201-1435; E-mail: pschwil@gwdg.de.

© 2002 by the Biophysical Society

0006-3495/02/09/1671/11 \$2.00

duplexes to transcription activator proteins (Rippe, 2000) and has proven particularly valuable in studying enzyme kinetics, where the specific endonucleolytic cleavage of a double-labeled substrate by *EcoRI* (Kettling et al., 1998) and other nucleases (Koltermann et al., 1998) has been investigated.

In spite of its obvious advantages for the analysis of molecular interactions, cross-correlation is still not widely applied in biophysical analysis. Reasons may be the greater efforts of introducing two rather than one properly labeled molecular species, but also the practical challenges of assembling a stable optical setup with maximum overlap of two illumination beams in a confocal fashion. Recently, a significant instrumental simplification has been introduced utilizing of two-photon excitation (Heinze et al., 2000). The underlying idea is the joint excitation of spectrally distinct fluorophores by a single infra-red (IR) illumination source, accomplished by the fact that two-photon excitation spectra, due to the different selection rules for this special kind of photophysical transition, differ considerably from their one-photon counterparts (Denk et al., 1990; Xu and Webb, 1997). Two-photon cross-correlation analysis has meanwhile been demonstrated with a large number of dye combinations (Schwille and Heinze, 2001; K. G. Heinze, in preparation) and has the potential to become a standard tool in the FCS field. It not only promises an attractive extension for more than two molecular species to be simultaneously probed, but also offers a considerably simplified method for intracellular dual-color applications, because two-photon FCS has already been shown to be superior in many respects for work in live cells or tissue (Schwille et al., 1999).

An important conceptual difference between single- and dual-color FCS analysis is the evaluation of measurement parameters. Although single-color autocorrelation analysis mainly focuses on characteristic time scales underlying the fluorescence fluctuations, and thus draws its fundamental information from the decay times and functional forms of autocorrelation curves in different modes of particle mobility and internal dynamics, the most important parameter for dual-color analysis is the amplitude of the cross-correlation function, which contains all required information about the existence and relative concentration of double-labeled particles (Schwille et al., 1997b; Schwille, 2001b). In principle, this amplitude reflects nothing else than the existence of temporal coincidences of fluctuations in the two simultaneously recorded fluorescence signals. The larger the number of joint fluctuations in both channels with respect to the number of fluctuations in each single channel, the higher the relative amplitude of the cross-correlation function with respect to the amplitudes of the autocorrelation curves (Heinze et al., 2000). Thus, instead of recording the full temporal correlation function containing all dynamic information about the fluctuation decay, a simplified mode of data analysis can be applied, focusing only on the cross-correlation amplitudes, or coincidence factors (Winkler et

al., 1999), without losing information about the kinetic process under study. In other words, if only relative concentrations—and their temporal evolution—of double-labeled species are of interest, as is the case for basically all standard FCS investigations of association–dissociation or enzyme kinetics, the simple assessment of cross-correlation amplitudes rather than decay functions is sufficient. This reduced amount of required information significantly simplifies the data processing procedure, leading to by far shorter measurement times. In addition to that, external perturbations can be applied to increase the number of fluctuation events at very low concentrations, e.g., by measuring in flowing sample streams or by probe scanning (Winkler et al., 1999; Bieschke et al., 2000). Fast relative movements of the sample with respect to the measurement volume, which would, in standard FCS, induce wrongly decreased fluctuation time scales, ideally do not alter the molecular concentrations, i.e., correlation amplitudes, and can thus be easily applied to enhance statistics for cross-correlation or coincidence measurements.

These features of enhanced statistics are of particular importance for the use of confocal techniques in screening applications, where short measurement times are required (Koltermann et al., 1998, 2001; Rarbach et al., 2001). Moreover, the reduction of measurement times emphasizes the attractiveness of FCS for intracellular studies on living systems, where the average applied illumination dose should be kept as small as possible, or for the investigations of fast association or dissociation processes that take place on a second's time scale and can thus not afford long recording times for each single data point. For this reason, the combination of fast dual-color coincidence analysis with two-photon excitation is straightforward and promises great advantages for many applications already opened up by the more general technique of two-photon cross-correlation spectroscopy (TPCCS). The present paper introduces the conceptual idea of two-photon coincidence analysis, outlining the crucial measurement parameters such as the coincidence value K and its standard deviation σ_K , and discusses the experimental limits with respect to a possible reduction of measurement times. Utilizing an established enzymatic test assay for endonuclease activity (Kettling et al., 1998), we specifically focus on the possibility of distinguishing positive from negative samples, as would be required for biotechnological screening purposes. It can be demonstrated that the data recording times to test for such distinctions can be reduced by two orders of magnitude to 100 ms and below, compared to times in the 10-s regime that are usually required for standard FCS and TPCCS analysis. Different dye combinations are evaluated and discussed with respect to their obtainable signal-to-noise (S/N) levels, mainly determined by their photochemical stability under two-photon excitation.

THEORETICAL CONCEPT

Dual-color cross-correlation and coincidence analysis

The detailed theoretical concept of cross-correlation analysis and the discussion of fundamental measurement parameters can be found elsewhere (Schwille et al., 1997b; Schwille, 2001b). The normalized fluctuation correlation function is generally defined by

$$G_{ij}(\tau) = \frac{\langle \delta F_i(t) \delta F_j(t + \tau) \rangle}{\langle F_i \rangle \langle F_j \rangle}. \quad (1)$$

For $i = j$, Eq. 1 describes the temporal autocorrelation of a single fluorescence signal. If fluctuations of two different signals ($i \neq j$), e.g., of spectrally distinct emission are recorded and to be compared, $G_{ij}(\tau)$ defines the cross-correlation function. Under ideal experimental conditions, the amplitude $G_{ij}(0)$ is directly proportional to the relative concentration of double-labeled molecules contributing to both signals F_i and F_j . Their absolute concentration can easily be derived if the corresponding autocorrelation amplitudes are simultaneously recorded (Heinze et al., 2000). Auto- and cross-correlation curves for particles with average concentrations $\langle C_i \rangle$, $\langle C_j \rangle$ and $\langle C_{ij} \rangle$ (double-labeled species) are then given by

$$G_{i,j}(\tau) = \frac{\langle C_{i,j} \rangle M_{i,j} + \langle C_{ij} \rangle M_{i,j}}{V_{\text{eff}} (\langle C_{i,j} \rangle + \langle C_{ij} \rangle)},$$

$$G_{ij}^{\times}(\tau) = \frac{\langle C_{ij} \rangle M_{ij}}{V_{\text{eff}} (\langle C_{i,j} \rangle + \langle C_{ij} \rangle) (\langle C_{j,i} \rangle + \langle C_{ij} \rangle)}, \quad (2)$$

with V_{eff} as the effective measurement volume element and $M_{i,j,ij}$ at the time-dependent correlation decay functions governed by molecular dynamics. For two-photon excitation, the effective volume size is $V_{\text{eff}} = (\tau/2)^{3/2} r_0^2 z_0$ with $1/e^2$ values r_0 and z_0 (Schwille et al., 1999). For noninteracting particles freely diffusing in 3D, M are given by

$$M_{i,j,ij}(\tau) = (1 + \tau/\tau_{d,i,j})^{-1} (1 + r_0^2 \tau / z_0^2 \tau_{d,i,j})^{-1/2}, \quad (3)$$

where $\tau_{d,n} = r_0^2 / 8D$ (for two-photon excitation) are defined as the average lateral diffusion times for a molecule of species i, j, ij with diffusion coefficient $D_{i,j,ij}$ through V_{eff} . For a known V_{eff} , the concentration of double-labeled species can be derived as follows from auto- and cross-correlation amplitudes without considering the molecular mobility,

$$\langle C_{ij} \rangle = G_{ij}(0) / (V_{\text{eff}} G_i(0) G_j(0)). \quad (4)$$

In the absence of double-labeled species, $G_{ij}(0)$ in principle equals zero for completely separable detection channels. Unfortunately, such a complete separation is hard to accomplish with a set of fluorescent probes in the visible spectral range. In reality, unspecific cross-talk, particularly due to

long-wavelength emission of the blue-shifted dye, cannot be neglected and has to be accounted for by determining the relative emission signals, in count rates per molecule, η , in both detection channels (Schwille et al., 1997b; Schwille, 2001b). In practice, this cross-talk induces a nonzero amplitude of the cross-correlation curve even if no double-labeled species is present. The general performance of a cross-correlation experiment is thus strongly dependent on the absolute difference in G_{ij} amplitudes between the positive (ideally only double-labeled species) and negative (ideally no double-labeled species) samples. This is exemplified in Fig. 1 A, comparing the cross-correlation results of an enzymatically digested double-labeled dsDNA sample together with its negative control, i.e., intact substrate. The positive sample is not reduced to zero because of two factors: cross-talk of the green label, and incomplete digestion of the substrate by the enzyme, further discussed elsewhere (Kettling et al., 1998; Heinze et al. 2000). The two curves clearly show the ability to distinguish positive from negative samples but also the possibility to resolve intermediate stages reflecting the kinetics of the digestion process. This is dependent both on the absolute difference in amplitudes $G(\tau)$ for every value τ and also the noise of the curve, i.e., the standard deviation of $G(\tau)$ values. This noise, in contrast, depends on the data-averaging process for any delay time τ . Because the standard hardware correlators for FCS utilize multiple- τ data processing, the sampling intervals for recording fluorescence raw data usually increase with τ . A determination of cross-correlation amplitudes will thus always involve a trade-off between larger discrepancies of fluctuation amplitudes at small τ , and lower noise of $G(\tau)$ values at large τ .

The experimental concept of confocal fluorescence coincidence analysis and two-photon fluorescence coincidence analysis is to record fluorescence signals with standard multi-channel scaler rather than correlator boards, and to use a relatively simple statistical algorithm for the quantitative comparison of fluctuations in the two measurement channels within a pre-defined sampling, or binning, time τ_b (Fig. 1 B). This very efficient mode of data evaluation has previously been described and tested successfully by Winkler et al. (1999). The chosen algorithm for fluctuation analysis utilizes the normalized product sum,

$$K(n) = \frac{\sum_{m=1}^n N_i(m) N_j(m)}{\sum_m N_i(m) \sum_m N_j(m)} \cdot n, \quad (5)$$

where the so-called coincidence value $K(n)$ represents the relative frequency of coincident events in the two detection channels. N_i and N_j are the absolute photon count numbers of the emission signals F_i and F_j in consecutive time channels m , each with sampling time τ_b . The overall analysis times T_m are given by the product of τ_b and the total number of time channels n . This kind of data recording reduces the read-out parameter $K(n)$ to a scalar value, and no further

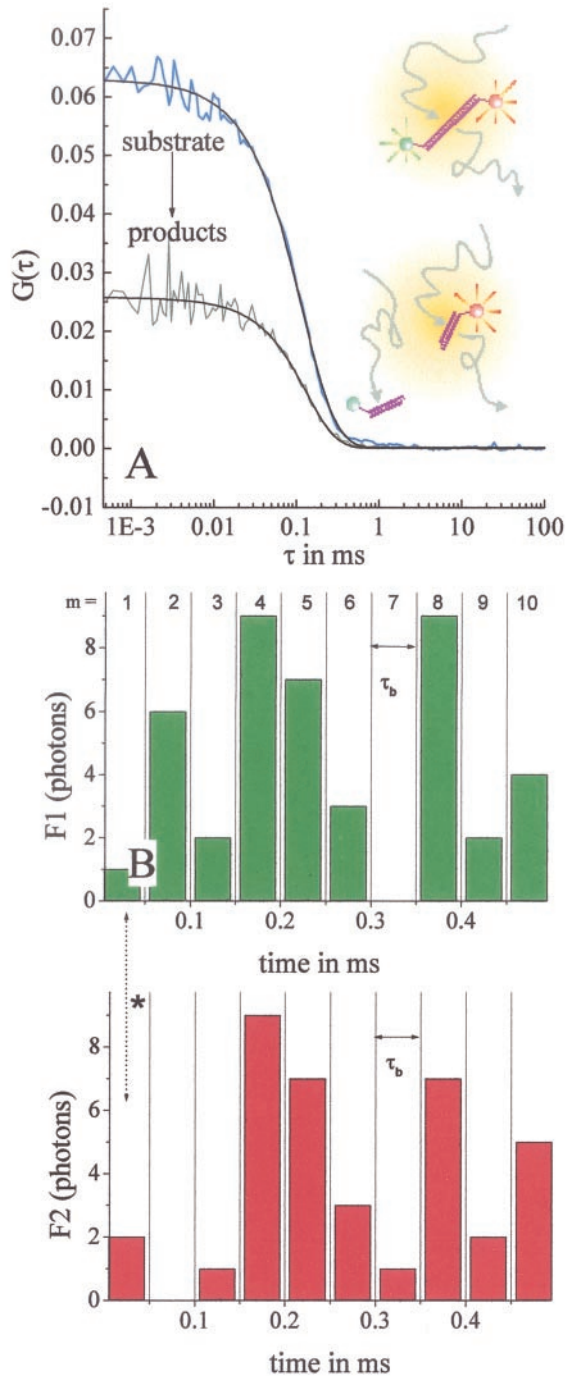


FIGURE 1 (A) Cross-correlation curves measured in confocal setup from a sample solution of 25 nM RhG/TR-labeled dsDNA target (top) and from an equivalent sample after *EcoRI* endonuclease treatment (bottom) representing the start and end points of the cleavage reaction. Fits according to Eq. 3 are shown. The difference in correlation amplitudes marks the dynamic performance of the setup. The data-collection time for each curve was 60 s. (B) Scheme of the statistical algorithm for the quantitative comparison of fluctuations in the two measurement channels within a pre-defined sampling time τ_b . The two raw-data fluorescence traces of channel 1 and channel 2 are sampled by τ_b and analyzed according to Eq. 5.

fitting procedure is required. Obviously, the standard deviation of $K(n)$, σ_K , reflecting the overall S/N levels, determines the possibility of separating different samples with respect to their concentration of double-labeled molecules. A series of $K(n)$ measurements usually results in a Gaussian distribution for the number of K events $D(K)$,

$$D(K) = D_{(K)} \exp(-(K - \langle K \rangle)^2 / 2\sigma_K^2). \quad (6)$$

Of particular importance in many applications of dual-color confocal fluorescence analysis, predominantly for screening purposes but also for analysis of cellular processes, is the clear distinction between positive and negative samples with respect to the existence of double-labeled molecules. We thus postulate a crucial requirement for the possible separation of two arbitrary cross-correlation amplitudes $G_{\times 1}(0)$ and $G_{\times 2}(0)$ (e.g., as in Fig. 1 A) at any stage of an association–dissociation process by introducing an additional separation quality parameter,

$$Q_{\text{sep}} = \frac{2|\langle K_1 \rangle - \langle K_2 \rangle|}{(\sigma_{K_1} + \sigma_{K_2})}, \quad (7)$$

where σ_{K_1} and σ_{K_2} are the standard deviations and $\langle K_1 \rangle$ the mean of the coincidence values $K_1(n)$ and $K_2(n)$ for two samples, 1 and 2, in a measurements series of n events as in Eq. 5. This value determines the relative distance of the two Gaussian-shaped distribution functions $D(K_1)$ and $D(K_2)$, with respect to their average broadness. Due to the above-discussed relationship between the absolute differences between $G_{\times 1}(\tau)$ and $G_{\times 2}(\tau)$ for any τ , and the standard deviations of the two values, there is an optimal sampling time τ_b that maximizes Q_{sep} . This optimal τ_b value strongly depends on the fluorescence assay used, i.e., the used dye combination, the detection efficiency, the amount of cross-talk between the detection channels, and, finally, the relative and absolute numbers of molecules under study. The scope of this study is to give guidelines how to determine optimal τ_b and consequently assess minimum data recording times T_m for the specific task of distinguishing positive from negative samples in a well-characterized enzymatic digestion assay. The applicability of the proposed TPFCA method is widespread and not limited to enzyme kinetics with simple yes–no decisions for screening purposes.

Two-photon excitation

Two-photon excitation is induced by quasi-simultaneous ($\sim 10^{-15}$ s) absorption within the cross-section of the dye molecule ($\sim 10^{-16}$ cm²). It was introduced by Denk et al. (1990) to the biomedical sciences, as an elegant alternative to confocal laser scanning microscopy. Due to the square dependence of the simultaneous two-photon absorption probability on illumination intensity, the effective excitation volumes are usually much smaller than in the standard one-photon case, minimizing phototoxic effects in irradi-

ated cells and tissue. This inherent spatial sectioning also minimizes probe depletion within the sample, considerably improving measurements in small compartments like living cells (Williams et al., 1994; Schwille et al., 1999). In addition, advantage can be taken of the experimental finding that two-photon excitation spectra are generally much broader than the corresponding one-photon spectra, allowing for a comfortable performance of multi-color experiments. Recently, we demonstrated that it is in fact possible to excite two spectrally largely distinct dyes with a single IR laser line, and still gain sufficient signal to do reliable single molecule analysis (Heinze et al., 2000).

The number of two-photon excited photons collected in any detection channel for discrete photon recording steps $m = 0, 1, 2, \dots$ with sampling intervals τ_b is given by

$$N_{ij}(m) = \frac{1}{2} \kappa_{ij} g_2 q_{ij} \sigma_{ij} \langle I_0(t) \rangle^2 \tau_b^{-1} \times \int_{m \cdot \tau_b}^{(m+1) \cdot \tau_b} \int_V S^2(r) \Omega_{ij}(r) C_{ij}(r, t) \cdot dV dt, \quad (8)$$

where $\langle I_0(t) \rangle$ is the average intensity at the geometrical focal point, g_2 is the second-order temporal coherence of the excitation (Xu and Webb, 1997), $S(r)$ is the dimensionless spatial distribution function of the focused light in the sample space, $\Omega_i(r)$ is the optical transfer function for the emission, C_i is the concentration of the fluorophore species i , q_i is its quantum efficiency, σ_i is its two-photon absorption cross-section, and κ_i is the wavelength-dependent collection efficiency of the setup. This expression can be simplified as

$$N_{ij}(m) = \eta_{ij} V_{\text{eff}} \tau_b^{-1} \int_{m \cdot \tau_b}^{(m+1) \cdot \tau_b} C_{ij}(t) dt, \quad (9)$$

combining all parameters that determine the average photon emission yield per single molecule per unit time into a single variable η_{ij} (Schwille et al., 1997b). The effective volume element is for two-photon excitation given by $V_{\text{eff},2\text{PE}} = (\pi/2)^{3/3} r_0^2 z_0$ with r_0 and z_0 as the radial and axial $1/e^2$ values of the emission intensity distribution, assumed to be 3D Gaussian. The discrete signal sampling in τ_b steps results in a temporal integration over the fluctuating local concentration $C_{ij}(t)$ in the small volumes V_{eff} due to Brownian motion of the particles.

The photon count rate η_{ij} , usually determined in kHz/molecule, has previously been shown (Koppel, 1974; Qian, 1990; Kask et al., 1997) to significantly affect the signal/noise ratios in FCS measurements and related confocal techniques. It is therefore of crucial relevance to optimize this parameter in both detection channels. For simultaneous two-photon excitation of two dyes, optimization of η_{ij} is performed by scanning both the excitation power and wave-

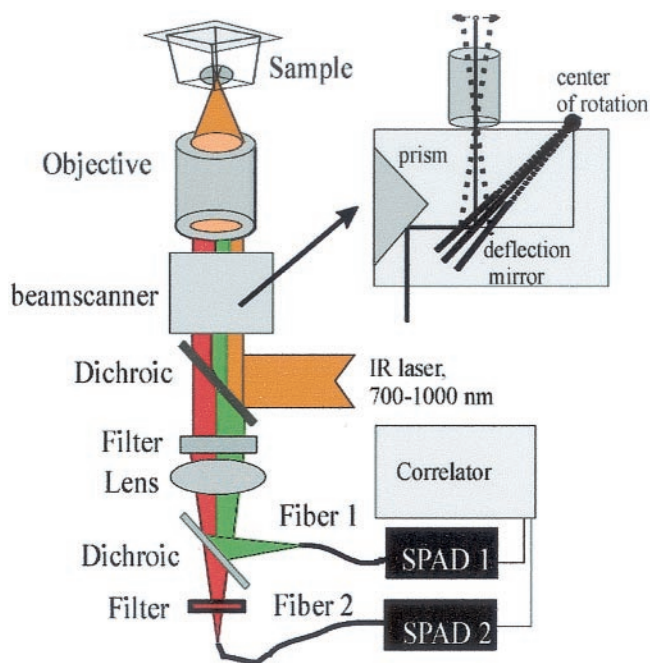


FIGURE 2 Optical setup for two-photon fluorescence coincidence analysis as realized in an inverted microscope Olympus IX70. A single tunable Ti:Sapphire laser line is used for illumination. The fluorescence emission is split by a dichroic mirror after the collimating lens and imaged onto two different optical fibers. The principle of the beam scanner is indicated in the inset: Between the dichroic mirror and the objective, a beam-deflection mirror is mounted to oscillate around a normal position by a galvanometer scanner, such that the excitation beam is scanned through a pivot point at the back of the objective.

length, and looking out for a good compromise in emission efficiencies (Heinze et al., 2000), with maximum signal and minimum bleaching from both selected dyes. In addition to that, fast scanning of the excitation beam, i.e., the measurement volume element through the sample has also been shown to dramatically reduce bleaching, and thus enhance η_{ij} (Winkler et al., 1999). Finally, different pairs of dyes can be used to guarantee high performance fluorescence assays. For that reason, the TPCCS assay under study will be optimized for all mentioned parameters.

MATERIALS AND METHODS

Experimental setup

The experimental setup (Fig. 2) is composed of an inverted Olympus IX-70 microscope and a fiber optics-coupled detection system. For two-photon excitation, a mode-locked femtosecond Ti:Sapphire laser beam (Spectra Physics, Mountain View, CA) epi-illuminates a water immersion objective (UPlanApo/IR 60xNA1.2, Olympus, Hamburg, Germany) via a dichroic mirror (710DCSPXR, AHF Analysentechnik, Tübingen, Germany). The emitted light is collimated and traverses a broadband emission filter (D600/200, AHF) for efficient suppression of IR light. Afterward, the remaining emission light is split by a second dichroic mirror (595 DCLP, AHF) into the red and green parts of the spectrum, whereupon the red part is additionally subject to long-pass filtering (RG610, Schott, Mainz, Ger-

many) to cut off nonspecific light from green fluorescent molecules reaching the red channel. Finally, the so-specified fluorescence is detected by two optical fiber-coupled avalanche photodiodes (SPCM-200, EG&G Optoelectronics, Vaudreuil, Canada). The optical setup has been described in detail for TPCC analysis by Heinze et al. (2000). In comparison to the earlier approach, for the present application, the specific filter for the green detector channel is missing, because higher emission yield in the green channel coming along with removing the filter is found to outmatch higher signal specificity in terms of data quality.

For coincidence measurements, the digital output pulses of the avalanche photodiodes are recorded and processed by an on-board processor PC card (Adwin 9LD, Jäger Messtechnik, Lorsch, Germany). Alternatively, the photon count signals could be processed and time correlated by an ALV-5000 multiple- τ correlator card (ALV, Langen, Germany). Evaluation of the auto- and cross-correlation curves was carried out by Origin (OriginLab, Northampton, MA) using Marquardt nonlinear least-square fitting routine.

Because coincidence analysis does not involve the evaluation of diffusional characteristics of the molecular species, statistical averaging may be improved by applying relative movements of sample and focal volume element. A beam-scanner device operating at frequencies up to 100 Hz developed by Evotec OAI (Hamburg, Germany, [Pat. No. WO9748001]) was used for these experiments. For all experiments, the deflection angle of the beam-scanner device is fixed to 1° , which is equivalent to a scanning range of $\sim 40 \mu\text{m}$.

Biochemical assay

The biochemical preparation of the test assay is similar to the system described by Ketting et al. (1998). Restriction endonuclease *EcoRI* (25 U/ μl) was purchased from Stratagene (Amsterdam, The Netherlands). Complementary oligonucleotides (66 nt) were custom synthesized both unmodified (MWG-Biotech, Ebersberg, Germany) and 5'-end-labeled with the red fluorescent dyes Alexa594 (A594) or Texas Red (TR) and green dyes Rhodamine green (RhG) or Alexa488 (A488) (Molecular Probes, Leiden, The Netherlands). Strands were annealed at 2.5 μM in 25 mM Tris-HCl (pH 7.5), 75 mM NaCl to yield dsDNA substrates with the dye combinations A594/A488 and TR/RhG. The endonucleolytic cleavage reaction was performed at 37°C for 1 h in digestion buffer (150 mM KOAc, 37.5 mM Tris-Acetate (pH 7.6), 15 mM MgOAc, 0.75 mM β -mercaptoethanol, 15 $\mu\text{g/ml}$ BSA, 0.05% Triton X-100) using 0.75 unit/ μl *EcoRI* and 1.25 μM dsDNA. Digestion studies were performed using 25 nM of double-labeled DNA substrate.

Dye system and calibration measurements

The selection of proper dye systems for dual-color applications is critically dependent on photostability, quantum yield, two-photon absorption spectra, and the spectral emission overlap of the respective dye pair. Comparable photostability of the dye system at a chosen two-photon wavelength is crucial because excitation intensity cannot be regulated independently. Based on experimental data of previous two-photon FCS measurements (Heinze et al., 2000), the primary dye combination selected for the following experiments is Rhodamine Green and Texas Red (RG/TR). The optimal excitation wavelength is 830 nm, where both dyes are excited equally well with fluorescence emission yields η_{max} of up to 13 kHz/molecule in both channels. Characterization and calibration measurements have been described in detail (Heinze et al., 2000). Additionally, comparable measurements for an alternative dye system consisting of Alexa 488 and Alexa 594 (A488/A594) have been carried out. Although the emission spectra are nearly identical to the RG/TR-combination (data not shown), optimal two-photon excitation of this system was found at 790 nm. The dyes show maximum two-photon fluorescence photon yields superior to the RG/TR combination, with $\eta_{\text{max}} = 20$ kHz/molecule in both channels.

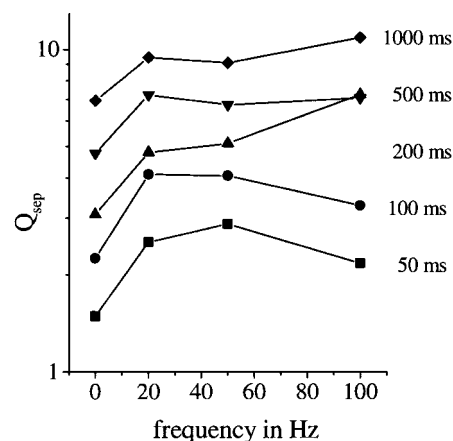


FIGURE 3 Separation quality Q_{sep} , according to Eq. 7, of each pair (cleaved and uncleaved sample) of coincidence data sets K (200 measurements each) as a function of the beam-scanner frequency at analysis times ranging from 50 to 1000 ms. The curves show similar behavior with a large improvement of Q_{sep} between 0 and 50 Hz. For short analysis times of 50 and 100 ms, a frequency of 50 Hz yields maximum performance.

This system has therefore been also selected as a promising dye combination for TPCFA assays.

RESULTS AND DISCUSSION

Relevant measurement parameters

A parameter of crucial relevance for many applications of TPCCS and TPFCA is the minimum total measurement time $T_m = n \times \tau_b$ to unambiguously distinguish two samples with different relative amounts of double-labeled species, their differences being predefined ratios for each system under study. For quantitative assessment, the separation parameter Q_{sep} (Eq. 7) between the two samples can then be determined for any given T_m , by fitting the K distributions in a series of single measurements, usually 100–200, according to Eq. 6. For enzyme assays, it is often sufficient to make simple yes–no decisions, to judge whether an enzyme is active at all. In this case, an appropriate separation parameter Q_{sep} must be determined for every substrate assay based on a positive and a negative control measurement. Generally, it is found that Q_{sep} strongly depends on measurement times $T_m = n \times \tau_b$ (Figs. 3 and 5), sampling times for data recording τ_b (Fig. 4), beam scanner frequency (Fig. 3), and finally, photostability and photon yields of the dye combinations (Figs. 6 and 7). To test the influence of any of these parameters on Q_{sep} , TPFCA measurements for positive (cleaved substrate) and negative (intact substrate) sample solutions of the endonuclease test assay were recorded. The results are discussed in detail below.

Influence of beam scanning

Beam scanning induces relative motion of the focal volume element with respect to the sample. As a consequence, the

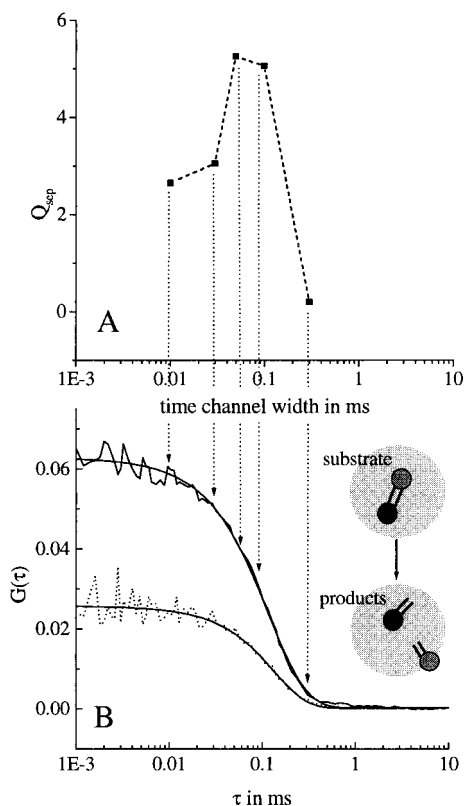


FIGURE 4 (A) Separation quality, Q_{sep} , dependent of the time channel width, τ_b , for each pair of coincidence K data sets (2×200 measurements, $T_m = 200$ ms) at 50-Hz beam-scanner frequency. (B) Correlation curves (40-s data recording) for comparison, to indicate the noise for τ_b . The optimal time channel width is found to be 50 μ s. For shorter times, the coincidence values are strongly scattered, whereas, for longer times, the collected photons become increasingly uncorrelated, both resulting in lower Q_{sep} .

number of single fluctuation events to be cross-correlated per unit time increases without changing the concentration, and the mean residence time of molecules in the focal region, and thus the probability of photobleaching, decreases. The influence of beam scanning frequency on Q_{sep} is exemplified for the RG/TR system in Fig. 3 with different total measurement times T_m at laser intensity of 30 mW, without photobleaching or saturation affecting the coincidence K (cf. Fig. 5). The scanning range is held constant in the described setup, where the frequency of scanning can be increased. As expected, Q_{sep} and thus, S/N increases significantly with T_m . It is also evident that the improvement of the S/N ratios at beam scanner frequencies lower than 50 Hz is substantial, compared with the stationary case. However, much higher frequencies do not further improve Q_{sep} , as the curves in Fig. 3 level off or even decrease. This fact can be attributed to many factors. It is likely that, at higher frequencies, mechanical perturbations of the measurement setup become apparent, which lowers the detection efficiency and increases the probability of detection artifacts. In

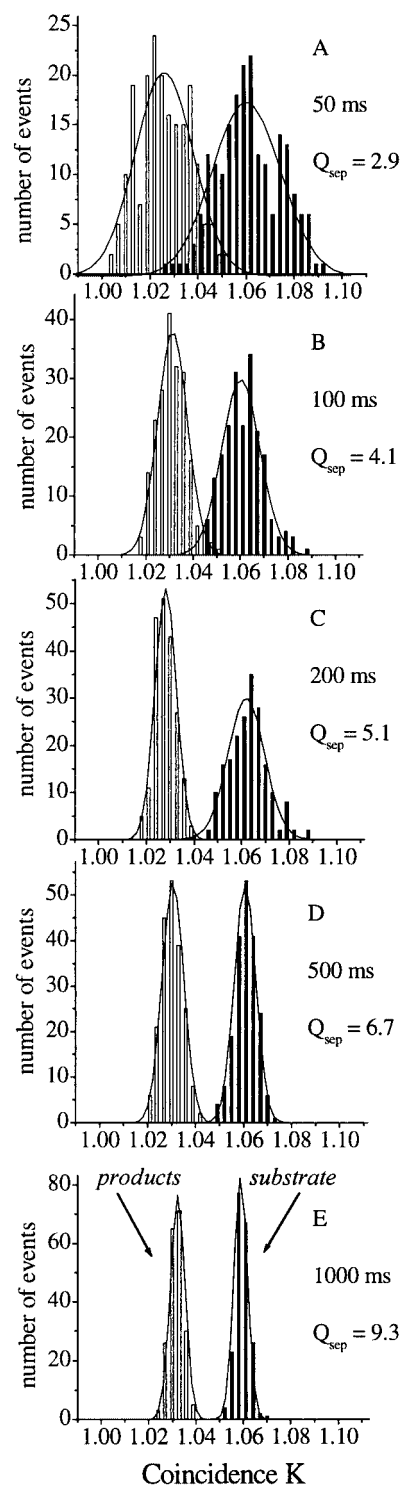


FIGURE 5 Histogram plots of 200 measurements of coincidence values K at 50-Hz beam-scanner frequency in samples of intact substrate (25-nM double-labeled dsDNA, gray bars) and the corresponding endonuclease-cleaved products (black bars). Plots A–E refer to different analysis times. The histograms were fitted by Gaussian distributions according to Eq. 6. As expected, separation quality, Q_{sep} , increases with increasing analysis time.

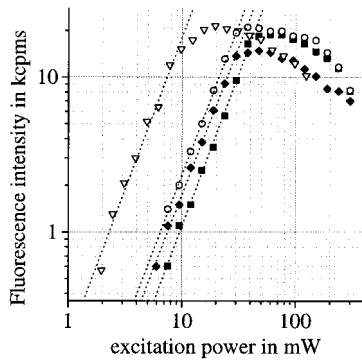


FIGURE 6 Fluorescence intensity of all used dyes (RG, TR, A488, A594) in kHz/s dependent on excitation power, plotted in double logarithmic scale. The excitation wavelengths are optimized for each dye independently (\circ , A488, 760 nm; \blacklozenge , RG, 800 nm; ∇ , A594, 800; \blacksquare , TR, 850 nm). The slope in the nonsaturated region is ~ 2 , as expected for TPE. Unlike the RG/TR dye system, the saturation levels for A488 and A594 are quite different. This difference is a disadvantage for excitation with a common excitation intensity. Note that the combination of A488 and TR would also yield poor results due to different excitation wavelengths required. In contrast to RG, the A488 cannot be excited efficiently close to the corresponding excitation maximum for its red counterpart TR at 850 nm.

contrast, if molecular residence times in the detection volume get too small, the photon statistics worsens as the probability of assigning two successive photon detection events to a single emitting molecule decays. We thus conclude that low frequencies below 50 Hz are preferable, the

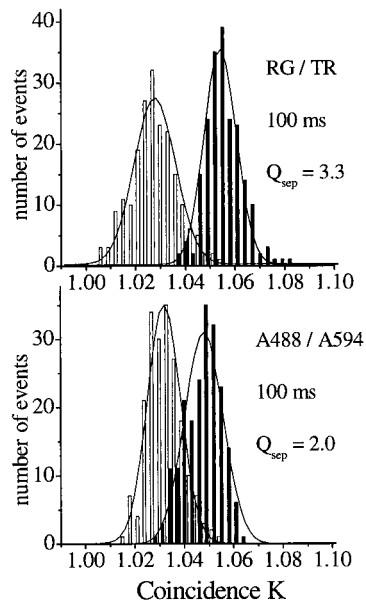


FIGURE 7 Histogram plots of the original RG/TR assay in comparison to an alternative A488/A594 assay. Each coincidence K plot is composed of 200 measurements at 50-Hz beam-scanner frequency in samples of intact substrate (*black bars*) and endonuclease-cleaved products (*gray bars*) as in Fig. 5. Although the spectral emission range is approximately the same for both dye systems, the resulting separation quality is significantly lower for the A488/A594 pair, because of the significantly different photostability of the two Alexa-dyes.

most dramatic increases of Q_{sep} , with respect to a stationary sample, can be expected up to 20 Hz. In the subsequent experiments, a beam-scanning frequency of 50 Hz has been chosen.

Influence of sampling times τ_b

The selection of proper τ_b is critical for good separability (large Q_{sep}) between two measurement curves, because two opposing effects have to be considered. Long sampling times evidently decrease the standard deviations of the measurements. This decreases the denominator (Eq. 7) of Q_{sep} . In contrast, shorter τ_b yield larger absolute differences in correlation amplitudes $G(\tau_b)$. A long τ_b thus decreases the numerator of Q_{sep} . Generally, τ_b should be smaller than the average diffusion time of the molecules through the measurement volume, to retain single-molecule specificity. Figure 4 quantifies the relationship between the separation quality of curves and the sampling time intervals by plotting Q_{sep} as a function of τ_b for a fixed beam scanner frequency of 50 Hz. The panel below exemplifies the concept by showing the respective $\tau = \tau_b$ values in a set of measured cross-correlation curves for cleaved and uncleaved substrate. For short $\tau = \tau_b$, Q_{sep} suffers from low confidence for the measurement of K values. The variance σ_K can be evidenced by the noise of the cross-correlation curves. For larger $\tau = \tau_b$, the signal quality increases. However, for $\tau_b > 0.1$ ms, where the magnitude of the diffusion time of molecules is reached or exceeded, collected photons become less correlated, resulting in worse separation quality. In our experimental setup with average particle residence times of 100 μs in the focal spot, the best compromise between low noise and a high yield of correlated photons is found for sampling times around 50 μs . This value maximizes separation efficiency of positive and negative samples. If lower beam scanning frequencies are applied, the range of optimal sampling times becomes broader, due to the correspondingly longer residence time of the molecule in the focal volume.

Distributions of coincidence factors K for different measurement times T_m

To illustrate the dependence of coincidence values K on the total measurement time T_m , histograms from a series of 200 measurements on positive and negative samples are depicted in Fig. 5. All measurements were carried out with a τ_b of 50 μs and a beam-scanner frequency of 50 Hz with the RG/TR assay. The resulting distribution histograms of K can be well approximated to be Gaussian (*solid lines*) according to Eq. 6. As expected, the separation parameter Q_{sep} , determined by the absolute distance of mean values and standard deviations of substrate and product distributions, increases with longer measurement times. No residual

overlap of the Gaussian distributions for analysis times larger than 200 ms is seen, reducing the possibility of false-positive or false-negative results to zero, if only single measurements would be taken. As a practical limit for fast screening purposes, analysis times of 100 ms are conceivable. For shorter analysis times, the overlap between the distributions becomes significant. Therefore, the measurement inaccuracy increases and a reliable discrimination of substrate and products by a single measurement can no longer be accomplished.

Assessing suitable dye pairs for dual-color TPCCS

Clearly, the dye pair RhG and TR chosen for the above studied fluorescent endonuclease assay is only one out of many different alternatives for fluorescent labeling in dual-color applications. Many other dye systems may be chosen if they fulfill the basic requirements, such as minimal overlap of emission spectra, similar emission characteristics for a common two-photon excitation wavelength, and comparable photostability. Photophysical characterization studies by our group (K. G. Heinze, unpublished data) have already revealed a large number of suitable dye combinations for dual-color two-photon applications, with the potential of more as new dyes are constantly introduced. To test an alternative dye pair as a reference for the measurements outlined above, an Alexa 488 and Alexa 594 based assay (A488/A594) for the same biochemical system was designed and evaluated. The wavelength at which both dyes are equally well excited is 790 nm, in contrast to 830 nm for the RhG/TR pair. Figure 6 shows a comparison of the fluorescence yields η in kHz/molecule for all four dyes at varying excitation power in double-logarithmic scale. The slope in the low intensity range is for all curves close to 2 (1.92–1.98), as expected for TPE. Note that these curves were recorded independently under optimal conditions for each pure dye system. For the dual-color DNA assays measured in the respective detection setups, η is reduced in both detection channels about a factor of 2–3 by quenching of the DNA, and by the filter and fiber optics to fully separate the emission signals.

Both Alexa dyes show slightly higher maximum emission yields η under optimum excitation conditions than the RG/TR dye pair (Fig. 6). However, A594 yields maximum emission at much lower intensities than the three other dyes, and consequentially shows saturation and photobleaching effects (decrease of the curve) before its green partner A488. Saturation for A488 is obtained at ~ 45 mW, while A594 is already saturated at ~ 25 mW. Thus, no optimal common excitation intensity can be found for both dyes. To take advantage of the maximal brightness of A488, a higher intensity must be used causing considerable bleaching in A594, thus increasing the probability of detection artifacts. In contrast, in the low intensity range where photobleaching

can be suppressed for both dyes, the emission yield of A488 is very poor. In contrast, intensity dependencies and saturation thresholds are similar for both dyes in the TR/RG system. Hence, it is much less difficult to find a favorable common excitation intensity where photobleaching-induced artifacts are minimized. Although the combination of A488 and TR according to Fig. 6 would be an obvious alternative to circumvent the bleaching problem, this dye pair is unable to be properly excited using a common excitation wavelength, and cannot be used.

To demonstrate that the S/N ratios and Q_{sep} parameters are indeed decreased for the A488/A594 alternative, Fig. 7 shows a comparison of K distributions for both dye systems for a fixed analysis time T_m of 100 ms ($\tau_b = 50 \mu\text{s}$, 50 Hz scanning frequency). The η values for the RG/TR dye system are 2 and 3 kHz/s, respectively, at the common excitation intensity of 30 mW, so that both dyes are not saturated or bleached; the η values for the A488/A594 system are 1.5 and 7 kHz/s at 15 mW, where the Alexa 594 dye is already saturated. Although the spectral emission range is approximately the same for both dye combination and the A488/A594 system can, under optimal conditions, yield higher emission, the separation quality of the positive and negative samples for coincidence analysis is significantly lower, because the distributions show a much larger overlap and a smaller difference of mean values.

We commonly find that fluorescent probes designed for the red spectral range should be excited at much lower intensity levels than the blue or green dyes to obtain sufficient photon yields for single-molecule detection. The above-mentioned signal limitations due to saturation and photobleaching of the red probe are therefore not fully avoidable for co-excitation of dual- or multicolor systems. For that reason, critical assessments of intensity dependencies, as in Fig. 6, are always required when designing proper dual-color assays for cross-correlation and coincidence analysis.

CONCLUSIONS

The concept of two-photon-excited dual-color fluorescence coincidence analysis has been outlined and experimentally demonstrated, utilizing a test assay to probe specific endonucleolytic cleavage of double-labeled DNA. The relevant parameters to unambiguously discriminate positive from negative samples have been discussed and experimentally determined. A clear improvement of S/N ratios, expressed as Q_{sep} parameters for coincidence K distributions, with total measurement time T_m could be observed as expected. Additionally, optimal sampling-time intervals τ_b and beam scanning frequencies could be assigned to minimize standard deviations of K values and thus maximize separation quality Q_{sep} . Although the measurements were focused on simple discrimination of positive samples from negative controls, as required for yes–no decisions in high through-

put screening applications, the same experimental conditions can be applied to enhance temporal resolution in measurements of molecular interactions, as used in common dual-color cross-correlation schemes (Schwille et al., 1997b; Schwille, 2001b).

In terms of detection efficiency, two-photon coincidence analysis of the mentioned assay system is found to be comparable to respective one-photon setups using two excitation laser lines, while preserving the simplified optical setup for two-photon excitation with a single excitation line and no need for pinhole adjustment. Short analysis times down to 100 ms, as demonstrated here, would permit a maximum screening throughput of more than 100,000 samples per day, combining all advantages of confocal single molecule analysis such as high sensitivity and statistical confidence, and low consumption of reagents.

As an outlook, two-photon excited coincidence analysis with its average measurement times of some 100 ms per sample will become a promising alternative to cross-correlation measurements, although dynamic information such as diffusion times and other characteristic fluctuation time scales will be sacrificed by this type of analysis. As a practical alternative for both, the more time-consuming cross-correlation and the much less specific image co-localization techniques, it will be particularly advantageous for measurements in cells and tissues where low illumination doses are required to prevent the biological system from photoinduced damage. With its comparably narrow time window for data recording, it can also be used to study interactions among molecular species that take place on a time range of seconds, too fast to be resolved by conventional correlation analysis.

We thank Andre Koltermann and Ulrich Kettling for helpful discussions, Karin Birkenfeld for assistance in sample preparation, and Sally Kim for proofreading the manuscript.

Financial support provided by the German Ministry for Education and Research (Biofuture grant No. 0311845) and Evotec BioSystems AG, Hamburg, Germany, is gratefully acknowledged.

REFERENCES

- Aragón, S. R., and R. Pecora. 1976. Fluorescence correlation spectroscopy as a probe of molecular dynamics. *J. Chem. Phys.* 64:1791–1803.
- Bieschke, J., and P. Schwille. 1997. Aggregation of prion protein investigated by dual-color fluorescence cross-correlation spectroscopy. *In* Fluorescent Microscopy and Fluorescent Probes. Vol. 2. J. Slavik, editor. Plenum Press, New York. 81–86.
- Bieschke, J., A. Giese, W. Schulz-Schaeffer, I. Zerr, S. Poser, M. Eigen, and H. Kretzschmar. 2000. Ultrasensitive detection of pathological prion protein aggregates by dual-color scanning for intensely fluorescent targets. *Proc. Natl. Acad. Sci. U.S.A.* 97:5468–5473.
- Bonnet, G., O. Krichinsky, and A. Libchaber. 1998. Kinetics of conformational fluctuations in DNA hairpin-loops. *Proc. Natl. Acad. Sci. U.S.A.* 95:8602–8606.
- Denk, W., J. H. Strickler, and W. W. Webb. 1990. Two-photon laser scanning fluorescence microscopy. *Science*. 248:73–76.
- Eigen, M., and R. Rigler. 1994. Sorting single molecules: Applications to diagnostics and evolutionary biotechnology. *Proc. Natl. Acad. Sci. U.S.A.* 91:5740–5747.
- Elson, E. L., and D. Magde. 1974. Fluorescence correlation spectroscopy. I. Conceptual basis and theory. *Biopolymers*. 13:1–27.
- Elson, E. L., and R. Rigler (Eds.). 2001. Fluorescence Correlation Spectroscopy. Theory and Applications, Springer, Berlin.
- Haupts, U., S. Maiti, P. Schwille, and W. W. Webb. 1998. Dynamics of fluorescence fluctuations in green fluorescent protein observed by fluorescence correlation spectroscopy. *Proc. Natl. Acad. Sci. U.S.A.* 95:13573–13578.
- Heinze, K. G., A. Koltermann, and P. Schwille. 2000. Simultaneous two-photon excitation of distinct labels for dual-color fluorescence cross-correlation analysis. *Proc. Natl. Acad. Sci. U.S.A.* 97:10377–10382.
- Kask, P., R. Günther, and P. Axhausen. 1997. Statistical accuracy in fluorescence fluctuation experiments. *Eur. Biophys. J.* 25:163–169.
- Kettling, U., A. Koltermann, P. Schwille, and M. Eigen. 1998. Real time enzyme kinetics of restriction endonuclease *EcoRI* monitored by dual-color fluorescence cross-correlation spectroscopy. *Proc. Natl. Acad. Sci. U.S.A.* 95:1416–1420.
- Kinjo, M., and R. Rigler. 1995. Ultrasensitive hybridization analysis using fluorescence correlation spectroscopy. *Nucleic Acids Res.* 23:1795–1799.
- Koltermann, A., U. Kettling, J. Bieschke, T. Winkler, and M. Eigen. 1998. Rapid assay processing by integration of dual-color fluorescence cross-correlation spectroscopy: high throughput screening for enzyme activity. *Proc. Natl. Acad. Sci. U.S.A.* 95:1421–1426.
- Koltermann, A., U. Kettling, J. Stephan, T. Winkler, and M. Eigen. 2001. Dual-color confocal fluorescence spectroscopy and its application in biotechnology. *In* Fluorescence Correlation Spectroscopy. Theory and Applications, E. L. Elson and R. Rigler, editors. Springer, Berlin. 87–203.
- Koppel, D. E. 1974. Statistical accuracy in fluorescence correlation spectroscopy. *Phys. Rev. A.* 10:1938–1945.
- Koppel, D. E., D. Axelrod, J. Schlessinger, E. L. Elson, and W. W. Webb. 1976. Dynamics of fluorescence marker concentration as a probe of mobility. *Biophys. J.* 16:1315–1329.
- Magde, D., E. L. Elson, and W. W. Webb. 1972. Thermodynamic fluctuations in a reacting system—measurement by fluorescence correlation spectroscopy. *Phys. Rev. Lett.* 29:705–708.
- Palmer, A. G., and N. Thompson. 1987. Molecular aggregation characterized by high order autocorrelation in fluorescence correlation spectroscopy. *Biophys. J.* 52:257–270.
- Qian, H. 1990. On the statistics of fluorescence correlation spectroscopy. *Biophys. Chem.* 38:49–57.
- Rabach, M., U. Kettling, A. Koltermann, and M. Eigen. 2001. Dual-color fluorescence cross-correlation spectroscopy for monitoring the kinetics of enzyme-catalyzed reactions. *Methods*. 24:104–116.
- Rigler, R., Ü. Mets, J. Widengren, and P. Kask. 1993. Fluorescence correlation spectroscopy with high count rates and low background: analysis of translational diffusion. *Eur. Biophys. J.* 22:169–175.
- Rigler, R., Z. Földes-Papp, F.-J. Meyer-Almes, C. Sammet, M. Völcker, and A. Schnez. 1998. Fluorescence cross-correlation—a new concept for polymerase chain reaction. *J. Biotechnol.* 63:97–109.
- Rippe, K. 2000. Simultaneous binding of two DNA duplexes to the NtrC-enhancer complex studied by two-color fluorescence cross-correlation spectroscopy. *Biochemistry*. 39:2131–2139.
- Schwille, P. 2001a. Fluorescence correlation spectroscopy and its potential for intracellular applications. *Cell. Biochem. Biophys.* 34:383–408.
- Schwille, P. 2001b. Cross-correlation analysis in FCS. *In* Fluorescence Correlation Spectroscopy. Theory and Applications, E. L. Elson and R. Rigler, editors. Springer, Berlin. 360–378.
- Schwille, P., J. Bieschke, and F. Oehlenschläger. 1997a. Kinetic investigations by fluorescence correlation spectroscopy: The analytical and diagnostic potential of diffusion studies. *Biophys. Chem.* 66:211–228.

- Schwille, P., U. Haupts, S. Maiti, and W. W. Webb. 1999. Molecular dynamics in living cells observed by fluorescence correlation spectroscopy with one- and two-photon excitation. *Biophys. J.* 77:2251–2265.
- Schwille, P., and K. Heinze. 2001. Two-photon fluorescence cross-correlation spectroscopy. *Chem. Phys. Chem.* 2:269–272.
- Schwille, P., and U. Kettling. 2001. Analyzing single protein molecules using optical methods. *Curr. Opin. Biotechnol.* 12:382–386.
- Schwille, P., F.-J. Meyer-Almes, and R. Rigler. 1997b. Dual-color fluorescence cross-correlation spectroscopy for multicomponent diffusional analysis in solution. *Biophys. J.* 72:1878–1886.
- Wallace, M. I., L. M. Ying, S. Balasubramanian, and D. Klenerman. 2000. FRET fluctuation spectroscopy: exploring the conformational dynamics of a DNA hairpin loop. *J. Phys. Chem. B.* 104:11551–11555.
- Weiss, S. 1999. Fluorescence spectroscopy of single biomolecules. *Science.* 283:1676–1683.
- Widengren, J., Ü. Mets, and R. Rigler. 1995. Fluorescence correlation spectroscopy of triplet states in solution: a theoretical and experimental study. *J. Chem. Phys.* 99:13368–13379.
- Widengren, J., and R. Rigler. 1998. Fluorescence correlation spectroscopy as a tool to investigate chemical reactions in solutions and on cell surfaces. *Cell. Mol. Biol.* 44:857–879.
- Widengren, J., E. Schweinberger, S. Berger, and C. A. M. Seidel. 2001. Two new concepts to measure fluorescence resonance energy transfer via fluorescence correlation spectroscopy: theory and experimental realizations. *J. Phys. Chem.* 105:6851–6866.
- Williams, R. M., D. Piston, and W. W. Webb. 1994. Two-photon molecular excitation provides intrinsic 3-dimensional resolution for laser-based microscopy and microphotochemistry. *FASEB J.* 8:804–813.
- Winkler, T., U. Kettling, A. Koltermann, and M. Eigen. 1999. Confocal fluorescence coincidence analysis. An approach to ultra high-throughput screening. *Proc. Natl. Acad. Sci. U.S.A.* 96:1375–1378.
- Xu, C., and W. W. Webb. 1997. Multiphoton excitation of molecular fluorophores and nonlinear laser microscopy. In *Topics in Fluorescence Spectroscopy*. Chap. 5. J. Lakowicz, editor. Plenum Press, New York.